Nature Environment and Pollution Technology
An International Quarterly Scientific Journal

p-ISSN: 0972-6268
(Print copies up to 2016)
e-ISSN: 2395-3454

Vol. 24 | No. 1 | Article ID B4103 | 2025

Original Research Paper

https://doi.org/10.46488/NEPT.2025.v24i01.B4103

Open Access Journal

Geostatistical Appraisal to Comprehend Hydrogeochemical Environment of Major Ions and Depiction of Groundwater Suitability from Part of Balaghat District (M.P.), Central India

Y. A. Murkute† and A. P. Pradhan
Postgraduate Department of Geology, Nagpur University, Law College Square, Nagpur-440001, India
†Corresponding author: Y. A. Murkute; yogmurkute@rediffmail.com

Abbreviation: Nat. Env. & Poll. Technol.
Website: www.neptjournal.com

Received: 26-09-2023
Revised: 30-10-2023
Accepted: 22-12-2023

Key Words:

Geostatistics
Hydrogeochemical environment
Groundwater quality

ABSTRACT

The key observations on the study concerning the geostatistical appraisal, hydrogeochemical environment of major ions (cations and anions) as well as groundwater suitability from the part of Balaghat District (MP) latitude 21°31'42": 21°43'11" N and longitude 79°50'30":80°11'30" E., Central India are presented here. The pH (7.3 to 8.6) of the groundwater samples and range of EC values (50-5080 $\mu S.cm^{-1}$) typically clarify the alkaline nature and the involvement of diverse processes (geogenic as well as anthropogenic) deciding the hydrogeochemical environment of groundwater. This prominent behavior is the result of the conductivity in groundwater, which is the consequence of ion exchange along with the solubilization processes during the rock-water interaction and also represents anthropogenic activity. The abundance succession of cations is $Ca^{2+} > Na^{+} > Mg^{2+} > K^{+}$, while the profusion sequence of anions is $HCO_3^- > Cl^- > NO_3^- > SO_4^{2-} > F^-$. The positive correlation among the pair of Ca^{2+} with Mg^{2+} (r = 0.657), Na^{+}(r = 0.691), and HCO_3^- (r = 0.842) as well as the high positive association between K^{+} and SO_4^{2-} (r = 0.856), plus K^{+} and NO_3^- (r = 0.779) unravels the derivation of ions from the geogenic origin and the agro-chemical derivation of ions respectively. The three factors (1:6.350, 2:2.732, and 3:2.697), having a total variance of 87.923%, correspond with the geogenic factor, anthropogenic factor, and alkalinity factor, respectively. The groundwater from the study area is suitable for drinking and irrigation purposes with a slight threat of exchangeable sodium.

Citation for the Paper:

Murkute, Y. A. and Pradhan, A. P., 2025. Geostatistical appraisal to comprehend hydrogeochemical environment of major ions and depiction of groundwater suitability from part of Balaghat District (M.P.), Central India. *Nature Environment and Pollution Technology*, 24(1), B4103. https://doi.org/10.46488/NEPT.2025.v24i01.B4103

Note: From year 2025, the journal uses Article ID instead of page numbers in citation of the published articles.

INTRODUCTION

The rock-water interface is the common intersection where the physical and chemical properties of both rocks, as well as groundwater, interact for the numerous crucial and decisive hydrogeochemical processes that directly govern the long-lasting chemistry of groundwater and hence also express the typical geogenic changes in the groundwater system (Sreedevi 2004, Nagaraju et al. 2006, Wen et al. 2008, Si et al. 2009, Deshpande & Murkute 2023). At this interface, distinct ions from the mineral suites get released from the aquifer rocks and also combine concurrently to give specific characteristics to the groundwater regime (Jalali 2006, Gupta et al. 2008, Murkute 2014a, Nayak & Hota 2023). Similarly, human interventions, which are also referred to as anthropogenic activities, add non-natural contents, which again deteriorate the groundwater quality (Si et al. 2009, Li et al. 2011, Ravikumar & Somashekhar, 2011, Agoubi et al. 2011, Rajesh et al. 2012, Omran et al. 2012, Bauder et al. 2014, Amiri et al. 2015, Xu et al. 2018, Ahada & Suthar 2018, Wagh et al. 2018, Zhang et al. 2019, Eyankware et al. 2020, Murkute 2014b).

Groundwater contamination poses an immense threat to human health, and hence the unfailing examinations have been expanding the apprehension of the hydrogeochemical environment through statistical investigations and other related

issues (Li et al. 2012, Brindha & Elango 2013, Wu et al. 2015, Hirojeet et al. 2015, Thilagavathi et al. 2015, Duraisamy et al. 2018, Sreedevi et al. 2018, Li et al. 2018, Xu et al. 2018, Adimalla & Qian 2019, Wang et al. 2019, Singh et al. 2019, Eyankware et al. 2020, Gogulothu et al. 2022). Nowadays, the interrelated studies give a hand in devising policies for planning, remedial measures, and regulations to cope with groundwater contamination.

The study area represents the western-south part of Balaghat district, latitude 21°31′42″: 2143′11″ N and longitude 79°50′30″: 80°11′30″ E, Madhya Pradesh, Central India. The study area also corresponds to five watersheds, wherein all these watersheds cover the rural part of the district, in which groundwater is the sole source of water for drinking and irrigation purposes. Seldom public water supply scheme provides tap water, but again the source of water is groundwater from shallow as well as deep aquifers. There is very little information available on the quality, statistical as well as geochemical characteristics of groundwater from this area. It is. Therefore, an endeavor has been made to investigate the hydrogeochemical behavior of groundwater by emphasizing the statistical methods, which would provide significant on groundwater quality. Hence, the statistical tools, namely factor, principal component, and cluster analyses, have been commenced to understand the various leading processes of groundwater chemistry (Hegeu & Kshetrimayum 2019, Ravish et al. 2020, Naidu et al. 2021, Natesan et al. 2022, Nayak & Hota 2023).

STUDY AREA

The Balaghat district is located in the southeastern part of Madhya Pradesh, Central India, and is bounded by Mandla, Rajnandgaon, and Seoni districts in the north, east, and west, respectively. The study area covers the western-south part of Balaghat district. It falls in degree sheet numbers 64B, 64C, 55O, and 55N between latitude 21°15' and 22°30' N and longitude 79°30' and 81°00' E (Fig.1). It represents the undulating area, where the semi-arid climatic condition prevails. In summer seasons, the utmost temperature blazes up to 45ºC and drops down in winter to 8ºC. The average annual rainfall is 1167 mm in the monsoon season, and humidity varies from 11 to 78%. The small streams of various orders delineate the dendritic-drainage pattern and drain out towards the northern part of the study area.

GEOLOGY AND HYDROGEOLOGY

The Archaean gneisses form the base of the geological set-up. These gneisses are coarse- to medium-grained and are composed mainly of plagioclase, quartz, and microcline with seldom biotite and hornblende mineral suites. The borewells located in this lithological unit have normal depth and diameters up to 60 meters below ground level (mbgL) and from 4 to 8 inches, respectively. The groundwater discharge is measured at 90 to 150 $m^3.day^{-1}$.

MATERIALS AND METHODS

In total, 77 groundwater samples were collected from preferred borewells, and the procedures precisely suggested by APHA (2012) were used for analytical measures. Respective field meters were utilized to measure the temperature, pH, and electrical conductivity (EC) at the borewell locations. The Ca^{2+}, Mg^{2+}, Cl^-, and HCO_3^- were counted by the titration method and the Na^+ K^+ concentrations were noted from the flame photometer. SO_4^{2-}, F^-, and NO_3^- were determined by

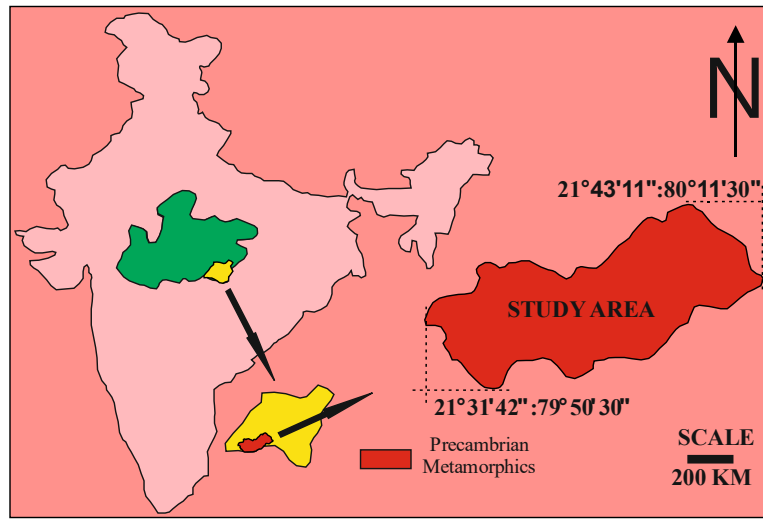

Fig. 1: Location map and geological map of the study area.

the UV-visible spectrophotometer. Total dissolved solids (TDS), as well as total hardness (TH), were worked out from mathematical expressions, and the concentrations of various ions have been presented in Table 1. The chloro-alkaline indices (CAI-1 and CAI-2) were determined after Schoeller (1977). The Principal Component Analysis (PCA) through Kaiser Normalization has been carried out after the standard procedure laid down by Hussain et al. (2016). Cluster analysis ramifies the variables into sets of comparatively homogeneous and distinct groups. Cluster analysis is carried out from correlation coefficient and Euclidean distances. The correlation coefficient method has been followed to group the groundwater parameters of the study area.

RESULTS AND DISCUSSION

Hydrogeochemistry of Ions

The pH and EC values were found to vary from 7.3 to 8.6 and 50 to 5080 $\mu S.cm^{-1}$ (Table 1), unraveling the alkaline nature and partaking of a multifarious series of processes in groundwater characterization (Subba Rao 2017). This highly elevated conductivity in groundwater is due to the ion exchange along with the solubilization processes during the rock-water interaction and may represent anthropogenic activity also (Sanchez-Perez & Tremolieres 2003, Choi et al. 2005). The high TDS (up to 3098 $mg.L^{-1}$, average value - 847.5 $mg.L^{-1}$) certainly represents the Geogenic as well as non-geogenic sources that contribute to salinity in the groundwater (Subba Rao et al. 2012).

In the groundwater samples of the study area, Ca^{2+} is found as the dominant constituent of the abundance succession of cations ($Ca^{2+} > Na^{+} > Mg^{2+} > K^{+}$). The concentration of Ca^{2+} varies from 8.0-493.0 $mg.L^{-1}$, while the Na^{+} content ranges from 4.2-540.0 $mg.L^{-1}$ (Table 1). The calcic plagioclases present in host rocks are the chief sources of $Ca^{2+,}$ and the dissolution of calcium-affluent mineral suites is the significant geogenic process responsible for the derivation of Ca^{2+} content in groundwater (Subba Rao & Chaudhary 2019, Murkute 2014b). Moreover, the loss of carbon dioxide as a result of changes in temperature and pressure conditions, reverse ion exchange as well and changes in precipitation cause the behavioral alteration in Ca^{2+} content in groundwater (Ahada & Suthar 2018, Nayak & Hota 2023). The preponderance of Na^{+} cation in groundwater points to the exhaustible weathering and dissolution of the host rocks as well as anthropogenic inputs. Also, the intake of such excessive concentration of Na^{+} than the permissible limit always poses a threat to the human body, causing the in-taker to be prone to cardiac, renal, and circulatory diseases (Mor et al. 2006). The concentration of Mg^{2+} varies from 4.9-332.9 $mg.L^{-1}$, while the K^{+} content ranges from 0.3-5.8 $mg.L^{-1}$. The Mg^{2+} is released from the mineral suites like mica, pyroxenes, amphiboles, magnesium calcite, traces of dolomite, and the gypsum resulting through the ion exchange processes (Thivya et al. 2018, Gogulothu et al. 2022). The at-par dominance of Mg^{2+} content conceivably points out the intense weathering of Mg-rich minerals from the host, suggesting the geogenic origin, contrary to the surplus use of fertilizers, pesticides, domestic wastes, septic tank spillages contribute to the anthropogenic inputs of Mg^{2+} in groundwater regime (Roy et al. 2018, Mgbenu & Egbueri 2019, Subba Rao 2021). The sodic plagioclases and potash feldspars (orthoclase and microcline) are the geogenic, while the potassium-based fertilizers, household wastes as well and irrigation-return-flows are the anthropogenic sources of K^{+} (Subba Rao et al. 2020).

HCO_3^- is the dominant anion with concentration varying from 20.0-516.0 $mg.L^{-1}$, and $HCO_3^- > Cl^- > NO_3^- > SO_4^{2-} > F^-$ is the order of abundance of the anions. HCO_3^- is formed by the release of CO_2 into the soil zone by the weathering of minerals, the influence of atmospheric $CO_{2,}$ and the decay of organic matter. Nevertheless, a higher concentration of HCO_3^- suggests the prevalence of mineral dissolution in the groundwater system (Subba Rao et al. 2021, Subba Rao 2018). The anthropogenic sources like domestic wastes, septic tank leakage, and irrigation-return-flow are the usual sources of Cl^- (8-1250.0 $mg.L^{-1}$) in the groundwater of the study area (Laxman et al. 2019).

The NO_3^- contents (0.8 – 541.9 $mg.L^{-1}$) have probably been released from the sewage waste, septic pool leakages, agricultural left-overs and decay of animal bodies (Subrahmanyam & Yadaiah 2000, Schilling & Wolter 2007, Raju et al. 2009, He et al. 2019). The SO_4^{2-} contents in groundwater of the present study area (0.6 – 184.0 $mg.L^{-1}$) possibly have been released through soil conditioners used in agricultural practices and from oxidation of sulfide minerals supplementary in fertilizers (Min et al. 2003, Chae et al. 2004, Subba Rao et al. 2012, Murkute 2014a). The F^- content varies from 0.5 - 1.5 $mg.L^{-1}$ with an average value of 1.0 $mg.L^{-1}$. The weathering of fluoride minerals like apatite, fluorite, biotite, hornblende, and phosphatic fertilizers are the chief sources of F^- in groundwater (Murkute 2014a, 2014b, Nayak & Hota 2023).

Geogenic and Non-Geogenic Source Genesis

The natural as well as human-induced processes are accountable for the generation of solute changes in the concentration of cations and anions, and the responsible processes may be categorized as rock weathering, evaporation as well and precipitation (Gibbs, 1970). Such Gibbs plots

Table 1: Range of cations and anions with desirable and permissible limits.

Sample No.	pH	EC	TDS	TA	TH	Ca^{2+}	Mg^{2+}	Na^{+}	K^{+}	HCO_3^{-}	Cl^{-}	SO_4^{2-}	F^{-}	NO_3^{-}	CAI-1	CAI-2
AP-1	7.70	488.00	312.00	160.00	236.1	64.10	18.50	23.00	1.60	160.00	35.00	8.20	0.820	6.23	0.3	0.0512
AP-2	7.80	284.00	186.00	128.00	99.8	24.00	9.70	14.40	1.50	128.00	10.00	1.80	0.760	5.83	-0.6	-0.042
AP-3	8.30	350.00	214.00	136.00	150.0	38.50	13.10	28.60	0.90	128.00	20.00	5.40	1.040	5.99	-0.5	-0.059
AP-4	8.20	2060.00	1214.00	516.00	598.6	56.10	111.80	144.00	1.60	516.00	225.00	120.00	1.180	26.64	0.4	0.0922
AP-5	7.60	2450.00	1520.00	408.00	1248.1	192.40	187.10	280.00	3.50	408.00	400.00	132.00	0.520	27.12	0.3	0.1239
AP-6	8.00	806.00	484.00	232.00	249.9	59.30	24.80	55.00	1.10	232.00	69.00	29.20	0.940	28.93	0.2	0.0391
AP-7	7.50	1160.00	672.00	344.00	459.7	85.00	60.30	62.00	1.80	344.00	90.00	62.40	1.040	51.24	0.3	0.0528
AP-8	7.70	1667.00	984.00	356.00	639.7	128.30	77.800	130.00	1.30	356.00	240.00	65.20	1.16	92.62	0.5	0.1644
AP-9	8.30	390.00	242.00	196.00	199.8	41.70	23.30	8.20	1.40	180.00	10.00	4.80	1.500	8.67	0.0	0.0019
AP-10	7.90	2050.00	1190.00	320.00	1018.7	176.40	140.90	214.00	1.80	320.00	300.00	104.40	0.940	34.29	0.3	0.1162
AP-11	8.40	773.00	510.00	364.00	299.4	48.10	43.70	25.60	1.60	348.00	38.00	7.80	1.320	34.21	0.3	0.0264
AP-12	7.30	3250.00	1982.00	360.00	1452.5	373.70	126.40	390.00	3.10	360.00	480.00	150.00	0.840	159.23	0.2	0.0878
AP-13	7.50	1321.00	792.00	280.00	540.2	160.30	34.00	120.00	2.40	280.00	160.00	56.40	0.660	85.72	0.2	0.0757
AP-14	7.90	950.00	560.00	220.00	400.2	112.20	29.20	66.00	1.80	220.00	110.00	32.80	0.740	50.76	0.4	0.1163
AP-15	8.20	1766.00	1024.00	320.00	839.4	168.30	102.10	130.00	1.50	320.00	220.00	80.60	0.860	126.12	0.4	0.1426
AP-16	8.30	709.00	460.00	344.00	363.3	62.50	50.50	19.50	2.00	336.00	26.00	8.80	1.120	5.52	0.2	0.0119
AP-17	7.90	1980.00	1228.00	380.00	839.5	176.40	97.20	190.00	3.60	380.00	260.00	65.40	0.800	94.59	0.3	0.0941
AP-18	8.40	858.00	498.00	200.00	320.3	112.20	9.70	72.00	2.50	176.00	95.00	28.00	1.160	37.68	0.2	0.0635
AP-19	7.90	247.00	160.00	88.00	140.1	25.70	18.50	13.80	0.80	88.00	20.00	7.80	0.940	9.10	0.3	0.0466
AP-20	7.80	50.00	34.00	20.00	40.1	8.00	4.90	4.20	0.30	20.00	8.00	0.60	0.700	1.97	0.4	0.1224
AP-21	8.60	683.00	396.00	260.00	300.1	80.20	24.30	22.20	1.20	236.00	35.00	24.20	1.300	15.57	0.3	0.0363
AP-22	7.80	1517.00	924.00	364.00	599.5	112.20	77.80	170.00	2.90	364.00	210.00	34.20	1.360	65.43	0.2	0.061
AP-23	8.20	1420.00	880.00	336.00	480.2	128.30	38.90	160.00	2.40	336.00	210.00	37.60	1.220	25.62	0.2	0.0816
AP-24	7.50	143.00	92.00	44.00	79.8	22.40	5.80	5.90	0.50	44.00	8.00	10.40	1.080	1.14	0.2	0.0256
AP-25	8.20	2160.00	1254.00	352.00	999.8	240.50	97.20	210.00	4.40	352.00	325.00	55.60	0.950	111.54	0.3	0.0512
AP-26	8.40	1235.00	766.00	240.00	519.3	96.20	68.00	110.00	3.40	224.00	150.00	32.80	1.180	86.71	-0.6	-0.042
AP-27	7.50	1160.00	684.00	368.00	459.8	104.20	48.60	76.00	2.40	368.00	110.00	11.40	1.250	29.32	0.3	0.151
AP-28	7.80	935.00	618.00	344.00	320.0	96.20	19.40	42.00	2.50	344.00	66.00	8.20	0.780	23.02	0.2	0.0866
AP-29	7.60	2740.00	1590.00	312.00	1019.4	224.40	111.80	270.00	4.80	312.00	550.00	108.00	1.220	20.89	0.3	0.0646
AP-30	7.70	2770.00	1690.00	352.00	1138.7	224.40	140.90	330.00	3.60	352.00	500.00	78.00	1.340	104.05	0.3	0.0514
AP-31	8.50	661.00	416.00	204.00	289.7	59.30	34.50	36.00	0.90	172.00	50.00	13.80	0.950	13.68	0.5	0.2837

Table Cont....

Sample No.	pH	EC	TDS	TA	TH	Ca^{2+}	Mg^{2+}	Na^{+}	K^{+}	HCO_3^{-}	Cl^{-}	SO_4^{2-}	F^{-}	NO_3^{-}	CAI-1	CAI-2
AP-32	8.20	1085.00	630.00	384.00	439.9	88.20	53.50	62.00	1.80	384.00	80.00	12.40	0.880	3.94	0.3	0.1789
AP-33	8.20	1241.00	732.00	320.00	479.6	101.00	55.40	82.00	2.40	320.00	122.00	32.60	0.620	49.19	0.3	0.0489
AP-34	7.80	579.00	354.00	280.00	239.9	49.70	28.20	64.00	1.60	280.00	50.00	3.40	0.940	1.58	0.2	0.034
AP-35	8.20	700.00	448.00	360.00	289.7	72.10	26.70	7.20	1.20	360.00	10.00	4.80	1.200	4.97	0.3	0.0792
AP-36	8.40	843.00	488.00	352.00	335.6	60.10	45.20	26.50	0.80	344.00	38.00	9.20	1.140	14.27	-0.3	-0.047
AP-37	8.20	670.00	402.00	260.00	319.7	57.70	42.80	16.70	0.70	260.00	23.00	8.20	1.380	7.88	0.2	0.0043
AP-38	8.20	670.00	402.00	260.00	319.7	57.70	42.80	16.70	0.70	260.00	23.00	8.20	1.380	7.88	0.3	0.0268
AP-39	8.10	447.00	260.00	88.00	180.0	49.70	13.60	36.50	0.50	88.00	53.00	6.60	0.780	12.22	0.2	0.0192
AP-40	7.70	688.00	440.00	280.00	335.7	64.90	42.30	18.60	1.40	280.00	25.00	8.80	0.640	8.91	0.2	0.0192
AP-41	7.90	1326.00	796.00	280.00	460.0	113.80	42.80	120.00	2.00	280.00	180.00	66.80	1.340	0.99	0.3	0.1084
AP-42	8.20	806.00	476.00	364.00	301.7	64.10	34.50	14.50	0.90	364.00	22.00	5.40	1.440	6.70	0.2	0.0159
AP-43	7.90	1610.00	966.00	320.00	723.3	129.90	97.20	144.00	2.80	320.00	196.00	40.00	0.920	68.38	0.3	0.1101
AP-44	8.00	1165.00	688.00	288.00	491.7	97.80	60.30	96.00	2.30	288.00	156.00	13.20	0.620	13.72	0.3	0.0169
AP-45	8.20	1525.00	886.00	276.00	240.1	65.70	18.50	82.00	3.10	276.00	125.00	32.00	0.720	2.56	0.3	0.0885
AP-46	7.40	1240.00	782.00	360.00	599.3	102.60	83.60	66.00	0.80	360.00	94.00	30.00	0.840	37.05	0.4	0.1262
AP-47	7.60	810.00	528.00	252.00	260.0	62.50	25.30	40.00	1.50	252.00	63.00	9.00	1.020	19.23	0.3	0.0921
AP-48	7.70	3440.00	1996.00	320.00	1496.3	200.00	243.00	360.00	3.50	320.00	550.00	120.00	0.740	382.30	0.3	0.0562
AP-49	7.60	3990.00	2354.00	360.00	1997.4	332.70	284.30	540.00	4.80	360.00	800.00	136.40	1.090	266.43	0.3	0.0664
AP-50	8.20	780.00	490.00	320.00	347.0	24.00	70.00	28.40	0.90	320.00	45.00	5.80	0.820	3.23	0.3	0.1884
AP-51	7.80	3510.00	2106.00	324.00	1298.0	200.40	194.40	390.00	4.50	324.00	600.00	62.60	1.260	226.23	0.3	0.1969
AP-52	7.90	5080.00	3098.00	340.00	1699.4	380.80	182.30	520.00	5.80	340.00	875.00	126.00	1.320	541.93	0.3	0.0423
AP-53	8.40	2690.00	1668.00	420.00	1047.6	80.20	206.60	260.00	3.20	412.00	350.00	92.40	0.900	119.81	0.3	0.2083
AP-54	8.20	688.00	400.00	288.00	249.8	41.70	35.50	22.80	2.50	288.00	30.00	6.20	0.740	5.91	0.4	0.2604
AP-55	8.00	3920.00	2274.00	288.00	1997.6	335.10	282.90	190.00	3.40	288.00	280.00	184.00	0.980	294.02	0.2	0.1006
AP-56	8.50	507.00	308.00	160.00	250.0	57.70	25.80	14.80	2.10	128.00	23.00	11.60	0.700	15.92	0.2	0.0145
AP-57	8.30	1804.00	1156.00	352.00	823.1	160.30	103.00	176.00	3.80	344.00	325.00	48.40	1.180	19.71	0.3	0.1152
AP-58	8.30	2920.00	1694.00	360.00	1098.9	224.40	131.20	292.00	4.20	352.00	525.00	130.20	1.220	117.84	0.3	0.0313
AP-59	8.10	4980.00	2938.00	300.00	2597.4	493.00	332.90	520.00	5.30	300.00	1250.00	180.00	0.820	219.92	0.4	0.2002
AP-60	8.30	1680.00	1024.00	236.00	619.5	120.20	77.80	210.00	2.20	228.00	325.00	54.60	0.600	29.95	0.4	0.2254
AP-61	8.50	520.00	328.00	228.00	250.0	52.10	29.20	8.10	0.80	204.00	10.00	4.20	0.860	0.79	0.6	0.4189
AP-62	8.30	890.00	544.00	268.00	359.4	65.70	47.60	72.00	1.40	260.00	95.00	14.60	0.880	3.78	0.3	0.1832
AP-63	8.20	313.00	204.00	100.00	189.7	32.10	26.70	12.50	0.60	100.00	17.00	7.00	0.700	12.65	0.1	0.0045

Table Cont....

Sample No.	pH	EC	TDS	TA	TH	Ca^{2+}	Mg^{2+}	Na^{+}	K^{+}	HCO_3^{-}	Cl^{-}	SO_4^{2-}	F^{-}	NO_3^{-}	CAI-1	CAI-2
AP-64	7.80	729.00	482.00	316.00	369.4	70.50	47.10	17.20	2.20	316.00	29.00	5.40	0.900	4.73	0.2	0.0572
AP-65	8.10	743.00	446.00	320.00	323.5	49.70	48.60	19.60	1.60	320.00	28.00	7.40	1.040	5.12	0.2	0.0315
AP-66	8.10	2760.00	1628.00	428.00	718.3	64.10	136.10	310.00	3.40	428.00	450.00	138.00	0.920	137.16	0.3	0.0274
AP-67	8.30	796.00	494.00	364.00	283.8	48.10	39.90	19.20	2.00	348.00	28.00	7.60	0.720	0.79	0.2	0.0191
AP-68	8.40	792.00	476.00	320.00	369.7	72.10	46.20	31.60	1.40	304.00	48.00	13.00	0.940	24.12	0.3	0.1344
AP-69	8.10	2410.00	1494.00	444.00	749.1	136.30	99.60	270.00	2.80	444.00	400.00	100.40	0.980	58.53	0.2	0.017
AP-70	8.40	626.00	388.00	240.00	239.9	43.30	32.10	25.00	1.40	216.00	33.00	12.60	1.240	9.77	0.3	0.0394
AP-71	8.10	623.00	374.00	260.00	247.6	44.10	33.50	17.80	0.60	260.00	25.00	11.80	0.740	3.15	0.3	0.1347
AP-72	8.50	1353.00	786.00	328.00	415.8	80.20	52.50	120.00	0.80	296.00	170.00	31.30	1.160	39.26	0.2	0.0231
AP-73	8.20	565.00	334.00	220.00	229.7	48.10	26.70	18.40	0.40	220.00	27.00	9.80	0.940	6.70	0.3	0.0222
AP-74	7.90	3050.00	1770.00	312.00	1159.8	288.60	106.90	320.00	1.80	312.00	480.00	24.40	0.820	299.54	0.3	0.093
AP-75	8.20	651.00	392.00	280.00	267.5	40.10	40.80	14.60	0.30	280.00	18.00	7.00	0.950	4.10	0.3	0.0319
AP-76	8.40	609.00	372.00	240.00	295.6	56.10	37.90	10.20	0.80	216.00	15.00	10.80	1.240	11.08	0.3	0.1938
AP-77	8.40	617.00	390.00	180.00	299.8	62.50	35.00	28.50	0.60	164.00	40.00	7.60	1.100	16.83	0.2	0.0102
Min	7.3	50.0	34.0	20.0	40.1	8.0	4.9	4.2	0.3	20.0	8.0	0.6	0.5	0.8	-	-
Max	8.6	5080.0	3098.0	516.0	2597.4	493.0	332.9	540.0	5.8	516.0	1250.0	184.0	1.5	541.9	-	-
Avg	8.0	1408.8	847.6	288.2	579.8	112.2	73.0	118.9	2.1	283.3	184.2	42.2	1.0	58.8	-	-
STDEV	0.3	1113.6	659.5	92.0	490.9	93.8	68.5	134.0	1.3	94.1	231.2	47.4	0.2	96.0	-	-
COV	3.9	79.0	77.8	31.9	84.7	83.6	93.8	112.7	62.4	33.2	125.5	112.4	23.7	163.2	-	-

Ions values are presented in $mg.L^{-1}$. SD – standard deviation, CV – covariance. DL – Desirable limit, PL – Permissible limit

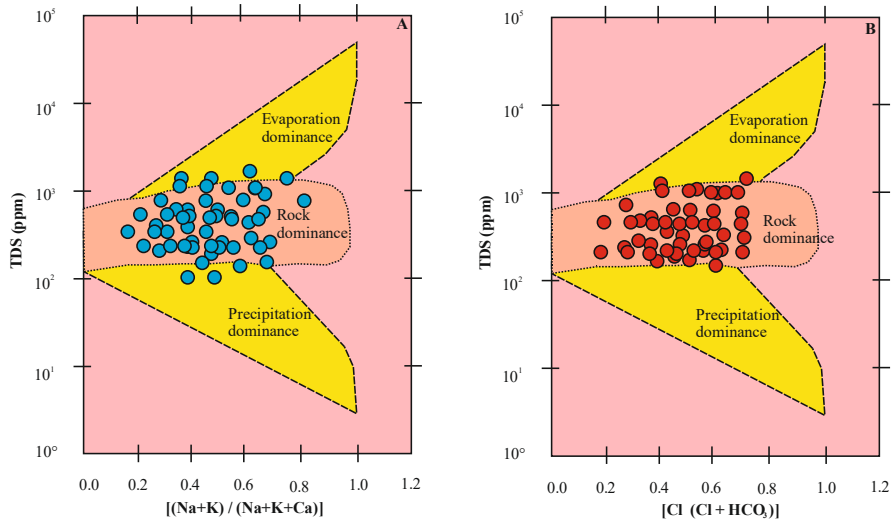

Fig. 2: Gibbs diagrams. a) TDS with [(Na+K) / (Na+K+Ca)], b) TDS with [(Cl/Cl+HCO_3)].

have been considered to discover the aforementioned responsible processes of the groundwater character from the study area (Fig. 2A, 2B). The Gibbs plots have been generated by plotting TDS with [(Na^++K^+)/(Na^++K^++Ca^{2+})] (Fig.2A) and TDS with [(Cl^-/Cl^-+HCO_3^-)] (Fig.2B) to assess the controlling sources of dissolved hydrogeochemical organization. The data points from these diagrams enumerate that the chemical weathering of rock-forming mineral suites is the key contributing feature in the evolution of the chemical composition of groundwater, which is secondarily influenced by anthropogenic activities (Gibbs 1970, Ravikumar et al. 2010).

The silicate weathering, revealed through reverse ion exchange or cation exchange, is the predominant process, which is governing the groundwater chemistry as revealed through the Cl^- vs. Na^+ plot (Fig. 3), wherein $Na^+ < Cl^-$ indicates reverse ion exchange, while $Na^+ > Cl^-$ suggests cation exchange (Subba Rao et al. 2019). This suggests that the silicate weathering resulting in cation exchange is the principal factor, while the reverse ion exchange is also an additional contributing factor to solute generation in the groundwater of the study area. For judging the sources of ions in groundwater, the chloro-alkaline indices (CAI-1) and (CAI-2) have been calculated, wherein the values of index CAI-1vary from -0.6 to 0.6, while the values of index CAI-2 range from -0.1 to 0.4 (Table 1). The inter-correlation of CAI-1 vs CAI-2 (Fig. 4) signifies the prevalence of cation exchange over reverse ion exchange.

The NO_3^- + Cl^-/HCO_3^- vs. TDS scatter diagram (Fig. 5) demonstrates a linear trend with a positive correlation, supporting the impact of non-geogenic sources

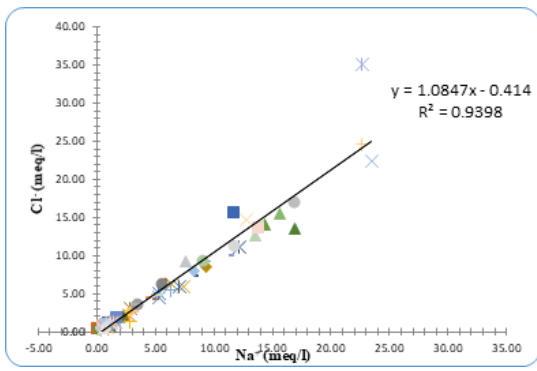

Fig. 3: Interrelation of Cl^- vs. Na^+ plot.

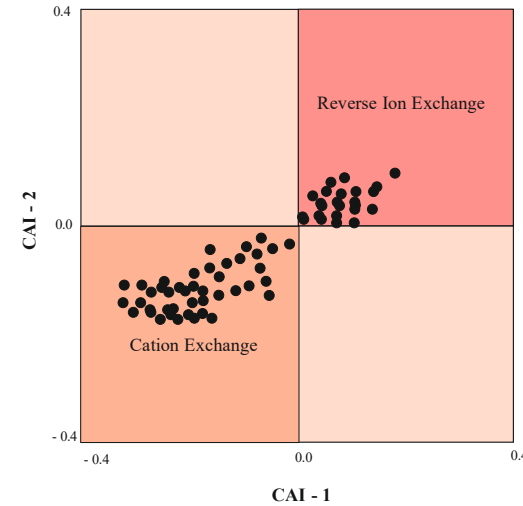

Fig. 4: Plot of CAI-1 vs. CAI-2 values calculated for groundwater samples from study area.

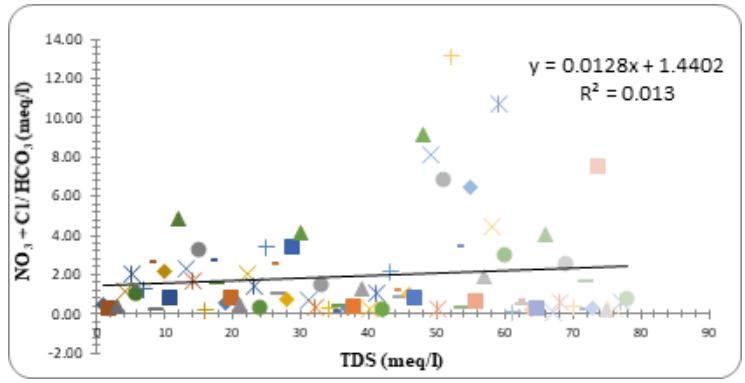

Fig. 5: plot of TDS vs. NO_3^-+Cl^-/HCO_3^- for groundwater samples from the study area.

Table 2: Pearson's bivariate correlation coefficients (r) between pairs of groundwater parameters.

	pH	TDS	TA	TH	Ca^{2+}	Mg^{2+}	Na^+	K^+	HCO_3^-	Cl^-	SO_4^{2-}	NO_3^-	F^-
pH	1.000	0.107	0.872**	0.048	0.198	-0.059	0.223	-0.011	0.127	0.192	-0.102	-0.183	0.878**
TDS		1.000	0.091	0.888**	0.856**	0.782**	0.877**	0.376*	0.876**	0.856**	0.481**	0.466**	0.174
TA			1.000	0.129	0.192	0.065	0.144	-0.167	0.221	0.117	-0.191	-0.252	0.808**
TH				1.000	0.879**	0.927**	0.679**	0.214	0.853**	0.689**	0.376*	0.345*	0.171
Ca^{2+}					1.000	0.657**	0.691**	0.189	0.842**	0.711**	0.265	0.166	-0.323*
Mg^{2+}						1.000	0.563**	0.184	0.709**	0.548**	0.446**	0.383*	0.071
Na^+							1.000	0.213	0.726**	0.945**	0.264	0.347*	0.314*
K^+								1.000	-0.063	0.214	0.856**	0.779**	-0.018
HCO_3^-									1.000	0.672**	0.013	0.019	0.231
Cl^-										1.000	0.285	0.264	0.294
SO_4^{2-}											1.000	0.799**	-0.061
NO_3^-												1.000	-0.167
F^-													1.000

on the groundwater chemistry of the study area (Li et al. 2019, Subba Rao et al. 2021). The important non-geogenic sources are unplanned irrigation-return-flow and the animal wastes sprawled throughout the study area, as well as the use of chemical fertilizers, soil conditioners, and manures in patchy agricultural fields.

Statistical Appraisal

The positive correlation of pH with TA (r = 0.872) and also with F^- (r = 0.878) discern strong involvement of the alkaline character of groundwater from the study area and the fluoride ion concentration (Table 2).

Such a positive phenomenon of TDS interrelationship with other ions suggests these ions are definitely the derived products of weathering and dissolution of mineral suites from the lithology and also the impact of anthropogenic activities (Subba Rao et al. 2020, 2021). The positive correlation among the Ca^{2+} with Mg^{2+} (r = 0.657), Na^+(r = 0.691), and HCO_3^- (r = 0.842) conveys the derivation of these ions from the similar lithological (geogenic) origin while the high positive correlations between K^+ and SO_4^{2-} (r = 0.856), as well as K^+ and NO_3^- (r = 0.779), puts on the derivation of these ions from the agro-chemical background (Nayak & Hota 2023).

In the factor analysis through Kaiser Criterion (Kaiser 1958), the 03 statistically significant factors out of all the variables have been found (Table 3), wherein three factors have eigenvalues of 6.350, 2.732, and 2.697, which account for 47.339%, 20.393% and 20.131% of variances respectively, with the total variance 87.923%. The factor-1, which is regarded as the geogenic factor, has very strong positive loadings on TDS (0.937), TH (0.923), Ca^{2+} (0.946), Mg^{2+} (0.906), Na^+ (0.838), HCO_3^- (0.947) and Cl^- (0.853), also corroborating the involvement of TDS, TH with

Table 3: Factor analysis data of groundwater parameters from the study area.

Groundwater parameters	Factor -1	Factor - 2	Factor - 3
pH	0.062	-0.031	**0.957**
TDS	**0.937**	0.315	0.072
TA	0.097	-0.192	**0.819**
TH	**0.923**	0.143	0.025
Ca^{2+}	0.946	0.077	0.151
Mg^{2+}	**0.906**	0.167	-0.101
Na^{+}	**0.838**	0.189	0.176
K^{+}	0.041	**0.961**	0.019
HCO_3^{-}	**0.947**	-0.182	0.068
Cl^{-}	0.853	0.151	0.134
SO_4^{2-}	0.168	**0.912**	-0.082
NO_3^{-}	0.217	**0.859**	-0.163
F^{-}	0.148	-0.051	**0.921**
Eigenvalues	6.350	2.732	2.697
Percentage of total variance	47.399	20.393	20.131
Cumulative percentage of total variance	47.399	67.791	87.923

three cations and two anions present in mineral suites of the host rocks. The ions in factor-2 loaded on K^{+} (0.961), SO_4^{2-} (0.912), and NO_3^{-} (0.859) are specifically present in fertilizers and soil conditioners used to enhance crop production and hence clearly be regarded as anthropogenic. The factor-3 strongly loaded with pH (0.957), TA (0.819), and F^{-} (0.921), is the alkalinity factor. The factor loadings in three-dimensional rotated space, evaluated for the present investigation, exemplify the ions-assemblage (Fig. 6) intimately resemble the findings of the factor analysis.

Groundwater Suitability

The suitability of groundwater for various purposes (drinking, as well as irrigation) has direct control on human health, household utility, furthermore agricultural soil, and crop fitness. The 69 % samples of the study area have EC values less than the permissible limit of 1500 $mg.L^{-1}$ (WHO (2017), suggesting suitability for drinking purposes. Considering TA (except sample 4: TA = 516 $mg.L^{-1}$) and TH content (31%), all the groundwater samples are suitable for drinking purposes. 55% of the samples from the study area have NO_3^{-} content more than the approved limits (WHO 2017, BIS 2020), hence specifying the need for proper sanitation measures as well as water purification. Sodium Adsorption Ratio (SAR), a test of irrigation suitability, represents the soil permeability, where in cations like Na^{+}, $Ca^{2+}$and Mg^{2+} ions are scientifically interconnected (SAR = $Na^{+}/\sqrt{[(Ca^{2+}+Mg^{2+})/2]}$). The SAR values pertaining to sodium hazard are compared with the salinity hazard (Fig. 7) in the US Salinity Laboratory's diagram (US Salinity Laboratory Staff 1954).

The bunch of plots of the samples in C_3-S_1 type denotes the water of medium to high salinity with medium sodium type. The 65% groundwater points corresponding to the C_3-S_2 and C_3- S_1 type unravel the medium salinity - medium sodium type. Both the above categories express the suitability of groundwater for irrigation purposes with a slight threat of exchangeable sodium. The other two minor clusters (C_4-S_2-10%, C_4-S_1 -5%) point out groundwater suitability for salt-tolerant or semi-tolerant crops.

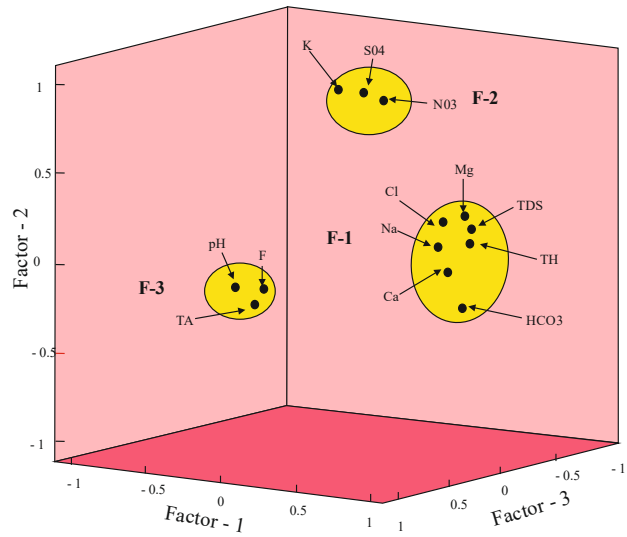

Fig. 6: Factor loadings in three-dimensional rotated space for groundwater samples from the study area.

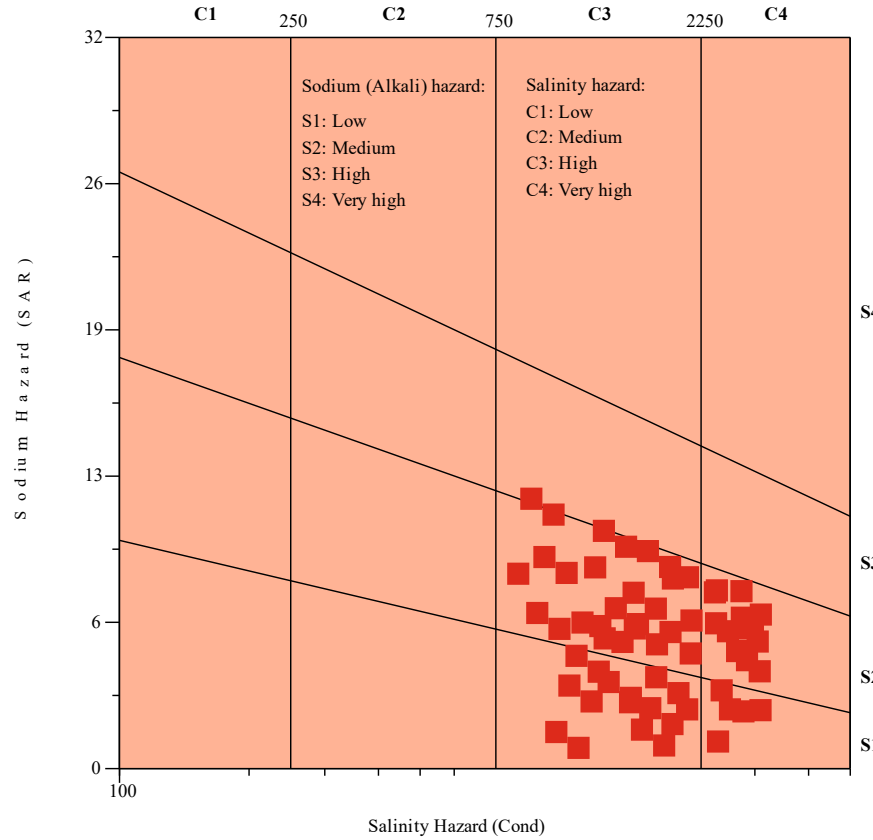

Fig. 7: US Salinity diagram for groundwater samples from the study area.

CONCLUSIONS

The key conclusions of the present study involving geostatistical appraisal, hydrogeochemical environment of major ions, and groundwater suitability from the part of Balaghat District (MP), Central India, are as follows:

i) The pH and EC values (7.3 to 8.6 and 50 to 5080 $\mu S.cm^{-1}$) illuminate the alkaline nature and multifarious processes in groundwater characterization. The prominent conductivity in groundwater represents the ion exchange along with the solubilization processes during the rock-water interaction and may represent anthropogenic activity also.

ii) The abundance succession of cations is $Ca^{2+} > Na^{+} > Mg^{2+} > K^{+}$, while HCO_3^- is dominant anion and abundance succession is $HCO_3^- > Cl^- > NO_3^- > SO_4^{2-} > F^-$. The calcic plagioclases present in host rocks are the chief sources of Ca^{2+}. The anthropogenic sources like domestic wastes, septic tank leakage, and irrigation-return-flow are the usual sources of Cl^- (8 – 1250.0 $mg.L^{-1}$) in the groundwater of the study area.

iii) The positive correlation among the Ca^{2+} with Mg^{2+} (r = 0.657), Na^{+}(r = 0.691), and HCO_3^- (r = 0.842) unravels the derivation of ions from the geogenic origin, whereas the high positive association between K^{+} and SO_4^{2-} (r = 0.856) as well as K^{+} and NO_3^- (r = 0.779) suggests agro-chemical derivation of ions.

iv) The eigenvalues of three factors (6.350, 2.732, and 2.697) have a total variance of 87.923%. The factor-1, factor-2, and factor-3 correspond with the geogenic factor, anthropogenic factor, and alkalinity factor, respectively.

v) The 69 % samples of the study area having EC values less than the permissible limit of 1500 $mg.L^{-1}$ suggests suitability for drinking purposes. The 65% groundwater points corresponding to the C_3-S_2 and C_3-S_1 types unravel the suitability of groundwater for irrigation purposes with a slight threat of exchangeable sodium.

ACKNOWLEDGMENTS

Authors extend special thanks to Dr. S.S. Deshpande and Ms. M.P. Jaunjalkar, PG Department of Geology RTMNU, Nagpur, for their technical support during the preparation of the manuscript and valuable suggestions.

REFERENCES

Adimalla, N. and Qian, H., 2019. Groundwater quality evaluation using water quality index (WQI) for drinking purposes and human health risk (HHR) assessment in an agricultural region of Nanganur, South India. *Ecotoxicology and Environmental Safety*, 176, pp.153–161.

Agoubi, B., Kharroubi, A. and Abida, H., 2011. Hydrochemistry of groundwater and its assessment for irrigation purposes in the coastal Jeffara aquifer, southeastern Tunisia. *Arabian Journal of Geosciences*, 6, pp.1163–1172.

Ahada, C.P.S. and Suthar, S., 2018. Assessing groundwater hydrochemistry of Malwa Punjab, India. *Arabian Journal of Geosciences*, 4, pp.11–17.

Amiri, V., Rezaei, M. and Sohrabi, N., 2014. Groundwater quality assessment using entropy weighted water quality index (EWQI) in Lenjanat, Iran. *Environmental Earth Sciences*, 72, pp.3479–3490.

APHA, 2012. WPCF, Standard methods for examination of water and wastewater. American Public Health Association/American Water Works Association/Water Environment Federation, Washington DC.

Bauder, T.A., Waskom, R.M., Sutherland, P.L. and Davis, J.G., 2014. *Irrigation Water Quality Criteria*. Colorado State University, p.506.

BIS, 2020. Indian standard drinking water specifications. IS: 10500, Edition 2.2 (2003-2009). Bureau of Indian Standards, New Delhi.

Brindha, K. and Elango, L., 2013. Geochemistry of fluoride-rich groundwater in a weathered granitic rock region, Southern India. *Water Quality Exposure and Health*, 5(3), pp.127–138.

Chae, G.T., Kim, K., Yun, S.T., Kim, K.H., Kim, S.O., Choi, B.Y., Kim, H.S. and Rhee, C.W., 2004. Hydrogeochemistry of alluvial groundwaters in an agricultural area: an implication for groundwater contamination susceptibility. *Chemosphere*, 55, pp.369–378.

Choi, B.Y., Yun, S.T., Yu, S.Y., Lee, P.K., Park, S.S., Chae, G.T. and Mayer, B., 2005. Hydrochemistry of urban groundwater in Seoul, South Korea: effect of land use and pollutant recharge. *Environmental Geology*, 48, pp.979–990.

Deshpande, S.S. and Murkute, Y.A., 2023. Hydrogeochemical characteristics and suitability of groundwater for drinking and irrigation from shallow aquifers of PG1 Watershed in Chandrapur District of Maharashtra. *Nature Environment and Pollution Research*, 22(2), pp.755–765.

Duraisamy, S., Govindhaswamy, V., Duraisamy, K., Krishinaraj, S., Balasubramanian, A. and Thirumalaisamy, S., 2018. Hydrogeochemical characterization and evaluation of groundwater quality in Kangayam taluk, Tirupur district, Tamil Nadu, India, using GIS tech. *Environmental Geochemistry and Health,* 18, p.183. https://doi.org/10.1007/s10653-018-0183-z.

Eyankware, M.O., Aleke, C.G., Selemo, A.O.I. and Nabo, P.N., 2020. Groundwater for sustainable development: hydrogeochemical studies and suitability assessment of groundwater quality for irrigation at Warri and environs, Niger delta basin, Nigeria. *Groundwater for Sustainable Development*, 10, pp.100293.

Gibbs, R.J., 1970. Mechanism controlling world water chemistry. *Science*, 17, pp.1088–1090.

Gogulothu, S., Subba Rao, N., Das, R. and Dhakate, R., 2022. Geochemical evaluation and suitability of groundwater quality for irrigation purposes in an agricultural region of South India. *Applied Water Science*, 12, p.142. https://doi.org/10.1007/s13201-022-01583-w.

Gupta, S., Mahato, A., Roy, P., Datta, J.K. and Saha, R.N., 2008. Geochemistry of groundwater, Burdwan district, West Bengal, India. *Environmental Geology*, 53, pp.1271–1282.

He, X., Wu, J. and He, S., 2019. Hydrochemical characteristics and quality evaluation of groundwater in terms of health risks in Luohe aquifer in Wuqi County of the Chinese Loess Plateau, Northwest China. *Human Ecology Risk Assessment*, 25, pp.32–51.

Hegeu, H. and Kshetrimayum, K.S., 2019. Hydrochemical characterization of groundwater in geomorphic units using graphical and multivariate statistical methods in Dimapur Valley, Northeast India. *Groundwater for Sustainable Development*, 8, pp.484–500.

Herojeet, R., Rishi, M.S. and Kishore, N., 2015. Integrated approach of heavy metal pollution indices and complexity quantification using chemometric models in the Sirsa Basin, Nalagarh valley, Himachal Pradesh, India. *Chinese Journal of Geochemistry*, 34, pp.620–633.

Hussin, N.H., Yusoff, I., Tahir, W., Mohamed, I., Ibrahim, A.I.N. and Rambli, A., 2016. Multivariate statistical analysis for identifying water quality and hydrogeochemical evolution of shallow groundwater in Quaternary deposits in the Lower Kelantan River Basin, Malaysian Peninsula. *Environmental Earth Sciences*, 75, p.1081. https://doi.org/10.1007/s12665-016-5705-3.

Jalali, M., 2009. Geochemistry characterization of groundwater in an agricultural area of Razan, Hamadan, Iran. *Environmental Geology*, 56, pp.1479–1488.

Kaiser, H.F., 1958. The varimax criterion for analytic rotation in factor analysis. *Psychometrika*, 23, pp.187–200.

Laxman, D.K., Satyanarayana, E., Dhakate, R. and Saxena, P.R., 2019. Hydrochemical characteristics concerning fluoride contamination in groundwater of Maheshwaram Mandal, RR District, Telangana state, India. *Groundwater for Sustainable Development*, 8, pp.474–483.

Li, P., Wu, Q. and Wu, J., 2011. Groundwater suitability for drinking and agricultural usage in Yinchuan area, China. *International Journal of Environmental Science*, 1(6), pp.1241–1249.

Li, P., Wu, J. and Qian, H., 2012. Groundwater quality assessment based on rough sets attribute reduction and TOPSIS method in a semi-arid area, China. *Environmental Monitoring and Assessment*, 184, pp.4841–4854.

Li, P., Wu, J., Tian, R., He, S., He, X., Xue, C. and Zhang, K., 2018. Geochemistry, hydraulic connectivity and quality appraisal of multilayered groundwater in the Hongdunzi coal mine, Northwest China. *Mine Water and the Environment*, 37, pp.222–237.

Li, P., He, X. and Guo, W., 2019. Spatial groundwater quality and potential health risks due to nitrate ingestion through drinking water: a case study in Yan'an City on the Loess Plateau of northwest China. *Human Ecology Risk Assessment*, 25, pp.11–31. https://doi.org/10.1080/10807039.2018.1553612.

Mgbenu, C.N. and Egbueri, J.C., 2019. The hydrogeochemical signatures, quality indices and health risk assessment of water resources in Umunya district, Southeast Nigeria. *Applied Water Science*, 9, pp.1–19.

Min, J.H., Yun, S.T., Kim, K., Kim, H.S. and Kim, D.J., 2003. Geologic controls on the chemical behavior of nitrate in riverside alluvial aquifers, Korea. *Hydrological Processes*, 17, pp.1197–1211.

Mor, S.K., Ravindra, R.P., Dahiya, P. and Chandra, A., 2006. Leachate characterization and assessment of groundwater pollution near municipal solid waste landfill site. *Environmental Monitoring and Assessment*, 118, pp.435–456.

Murkute, Y.A., 2014a. Hydrogeochemical characterization and quality assessment of groundwater around Umrer Coal Mine area, Nagpur District, Maharashtra, India. *Environmental Earth Sciences*, 72, pp.4059–4073.

Murkute, Y.A., 2014b. Hydrogeochemical behavior and groundwater suitability of Vislon Area, part of WRD Watershed, Chandrapur District, Maharashtra, India. *Pollution Research*, 42(1), pp.94–104.

Nagaraju, A., Arveti, M.R.S., Sarma, J.A., Aitkendead-Peterson, K. and Sunil, 2011. Fluoride incidence in groundwater: a case study from Talupula, Andhra Pradesh, India. *Environmental Monitoring and Assessment*, 172, pp.427–443.

Naidu, S., Gupta, G., Singh, R., Tahama, K. and Erram, V.C., 2021. Hydrogeochemical processes regulating the groundwater quality and its suitability for drinking and irrigation purpose in parts of coastal Sindhudurg district, Maharashtra. *Journal of the Geological Society of India*, 97, pp.173–185.

Natesan, D., Sabarathinam, C., Kamaraj, P., Mathivanan, M., Haji, M., Viswanathan, P.M., Chandrasekaran, T. and Rajendran, T., 2022. Impact of monsoon shower on the hydrogeochemistry of groundwater along

the lithological contact: a case study from South India. *Applied Water Science*, 12, pp.1–20.

Nayak, M. and Hota, R.N., 2023. Statistical evaluation of major ion chemistry of premonsoon groundwater of Kantapara Block, Cuttack District, Odisha. *Vist Geological Research*, 19, pp.46–56.

Omran, E.S.E., 2012. A proposed model to assess and map irrigation water well suitability using geospatial analysis. *Water*, 4, pp.545–567.

Rajesh, R., Brindha, K., Murugan, R. and Elango, L., 2012. Influence of hydrogeochemical processes on temporal changes in groundwater quality in a part of Nalgonda district, Andhra Pradesh, India. *Environmental Earth Sciences*, 65, pp.1203–1213.

Raju, N.J., Ram, P. and Dey, S., 2009. Groundwater quality in the lower Varuna River basin, Varanasi district, Uttar Pradesh, India. *Journal of the Geological Society of India*, 73, pp.178–192.

Ravikumar, P. and Somashekar, R.K., 2011. A geochemical assessment of coastal groundwater quality in the Varahi river basin, Udupi District, Karnataka State, India. *Arabian Journal of Geosciences*, 6, pp.1855–1870. https://doi.org/10.1007/s12517-011-0470-9.

Ravikumar, P., Venkatesharaju, K., Prakash, K.L. and Somashekhar, R.K., 2010. Geochemistry of groundwater and groundwater prospects evaluation, Anekal Taluk, Bangalore urban district, Karnataka, India. *Environmental Monitoring and Assessment*, DOI: 10.1007/s10661-010-1721-z.

Ravish, S., Setia, B. and Deswal, S., 2020. Groundwater quality analysis of northeastern Haryana using multivariate statistical techniques. *Journal of the Geological Society of India*, 95, pp.407–416.

Roy, A., Keesari, T., Mohokar, H. and Bitra, S., 2018. Assessment of groundwater quality in hard rock aquifer of central Telangana state for drinking and agriculture purposes. *Applied Water Science*. https://doi.org/10.1007/s13201-018-0761-3.

Sanchez-Perez, J.M. and Tremolieres, M., 2003. Change in groundwater chemistry as a consequence of suppression of floods: The case of the Rhine floodplain. *Journal of Hydrology*, 270, pp.89–104.

Schilling, K.E. and Wolter, C.F., 2007. A GIS based groundwater travel time model to evaluate stream nitrate concentration reductions from land use change. *Environmental Geology*, 53, pp.433–443.

Schoeller, H., 1977. Geochemistry of groundwater. In Brown, R.H., Konoplyantsev, A.A., Ineson, J., Kovalevsky, V.S. (eds.), Groundwater studies—An international guide for research and practice, Chapter 15, UNESCO, Paris, pp.1–18.

Si, J., Feng, Q., Wen, X., Su, Y., Xi, H., Chang, Z. and Li, Y., 2009. Major ion chemistry of groundwater in the extreme arid region northwest China. *Environmental Geology*, 57, pp.1079–1087.

Singh, G., Rishi, M.S., Herojeet, R., Kaur, L., Sharma, K. and Gupta, A., 2019. Evaluation of groundwater quality and human health risks from fluoride and nitrate in the semi-arid region of northern India. *Environmental Geochemistry and Health*. https://doi.org/10.1007/s10653-019-00449-6.

Sreedevi, P.D., 2004. Groundwater quality of Pageru River basin, Cuddapah District, Andhra Pradesh. *Journal of the Geological Society of India*, 64, pp.619–636.

Sreedevi, P.D., Sreekanth, P.D., Ahmed, S., Reddy, D.V. and Kumar, P., 2018. Appraisal of groundwater quality in a crystalline aquifer: A chemometric approach. *Arabian Journal of Geosciences*. https://doi.org/10.1007/s12517-018-3480-z.

Subba Rao, N. and Chaudhary, M., 2019. Hydrogeochemical processes regulating the spatial distribution of groundwater contamination, using pollution index of groundwater (PIG) and hierarchical cluster analysis (HCA): A case study. *Groundwater for Sustainable Development*. https://doi.org/10.1016/j.gsd.2019.100238.

Subba Rao, N., Subrahmanyam, A., Ravi Kumar, S., Srinivasulu, N., Babu Rao, G., Surya Rao, P. and Venktram Reddy, G., 2012. Geochemistry and quality of groundwater of Gummanampadu Sub-basin, Guntur District, Andhra Pradesh, India. *Environmental Earth Sciences*, 67, pp.1451–1471.

Subba Rao, N., Srihari, B., Spandana, D., Sravanthi, M., Kamalesh, T. and Abraham Jayadeep, V., 2019. Comprehensive understanding of groundwater quality and hydrogeochemistry for the sustainable development of suburban area of Visakhapatnam, Andhra Pradesh, India. *Human Ecological Risk Assessment*. https://doi.org/10/1080/10807039/1571403.

Subba Rao, N., 2017. *Hydrogeology - Problems with solutions*. PHI Learning Pvt. Ltd., Delhi, 265p.

Subba Rao, N., 2018. Groundwater quality from a part of Prakasam district, Andhra Pradesh, India. *Applied Water Science*, 8, p.30. https://doi.org/10.1007/s13201-018-0665-2.

Subba Rao, N., Ravindra, B., Wu, J. and Liu, Q., 2020. Geochemical and health risk evaluation of fluoride-rich groundwater in Sattenapalle Region, Guntur district, Andhra Pradesh, India. *Human Ecological Risk Assessment*, 26, pp.316–348.

Subba Rao, N., Dinakar, A., Sravanthi, M., Kumari, B.K. and Reddy, R., 2021. Geochemical characteristics and quality of groundwater evaluation for drinking, irrigation, and industrial purposes from a part of hard rock aquifer of South India. *Environmental Science and Pollution Research*, 28, pp.31941–31961.

Subrahmanyam, K. and Yadaiah, P., 2000. Assessment of the impact of industrial effluents on water quality in Patancheru and environs, Medak district, Andhra Pradesh, India. *Hydrogeology Journal*, 9(3), pp.297–312.

Thilagavathi, N., Subramani, T., Suresh, M., Karunanidhi, D. and Ramasamy, R., 2015. Mapping of groundwater potential zones in Salem Chalk Hills, Tamil Nadu, India, using remote sensing and GIS techniques. *Environmental Monitoring and Assessment,* 10, p.65. https://doi.org/10.1007/s10661-015-4376-y.

Thivya, C., Chidambaram, S., Thilagavathi, R., Venkatraman, G., Ganesh, N., Panda, B., Prasanna, M.V. and Kumar, V., 2018. Short-term periodic observation of the relationship of climate variables to groundwater quality along the KT boundary. *Journal of Climate Change*, 4, pp.77–86.

US Salinity Laboratory Staff, 1954. *Diagnosis and Improvements of Saline and Alkali Soils*. US Department of Agriculture Handbook, p.160

Wagh, V., Panaskar, D., Aamalawar, M. and Patil, V., 2018. Hydro-chemical characterization and groundwater suitability for drinking and irrigation uses in the semiarid region of Nashik, Maharashtra, India. *Hydrospatial Analysis*, 2, pp.43–60.

Wang, L., Mei, Y., Yu, K. and Zhang, W., 2019. Anthropogenic effects on hydrogeochemical characterization of the shallow groundwater in an arid irrigated plain in northwestern China. *Water*. 9, p.471. https://doi.org/10.3390/w11112247.

Wen, X.H., Wu, Y.Q., Wu, J. and Yang, X., 2008. Hydrochemical characteristics of groundwater in the Zhangye Basin, Northwestern China. *Environmental Geology*, 55, pp.1713–1724.

WHO, 2017. *Guidelines for Drinking Water Quality, Volume 1: Incorporating the First and Second Addenda, Recommendations*. WHO

Wu, J., Li, P. and Qian, H., 2015. Hydrochemical characterization of drinking groundwater with special reference to fluoride in an arid area of China and the control of aquifer leakage on its concentrations. *Environmental Earth Sciences*, 73, pp.8575–8588.

Xu, Y., Dai, S., Meng, K., Wang, Y., Ren, W., Zhao, L., Christie, P., Teng, Y. and Liu, H., 2018. Occurrence and risk assessment of potentially toxic elements and typical organic pollutants in contaminated rural soils. *Science of the Total Environment*, 630, pp.618–629.

Zhang, Y., Wu, J., Xu, B. and Li, S., 2018. Human health risk assessment of groundwater nitrogen pollution in Jinghui canal irrigation area of the Loess Plateau, northwest China. *Environmental Earth Sciences*, 77, pp. 273–283.